Supporting Information

Onishi et al. 10.1073/pnas.1000102107

SI Materials and Methods

DNA Constructs. Most of the cDNA constructs used in this study have been described previously (1). CAG-*ERR*β (estrogen-related receptor β) is generated by PCR using cDNA-specific primers for mouse *ERR*β and inserted into pCAGIG vector. The *ERR*β-VP16 fusion constructs were made by ligating the DNA-binding domain of *ERR*β (85–197 aa) to the transcriptional activator domain of the VP16 protein of herpes virus, followed by subcloning into pCAGIG vector (2).

Immunohistochemistry and in Situ Hybridization. Protocols for section immunohistochemistry and dissociated cell immunohistochemistry were performed as previously described (1), with the following exceptions. Additional antibodies were rabbit anti-*ERR*β (a gift from J. Nathans, Johns Hopkins University School of Medicine, Baltimore; 1:100 dilution), mouse anti-Lhx1 (4F2; Developmental Studies Hybridoma Bank; 1:200), mouse *ERR*α (Perseus Proteomics; 1:100), mouse *ERR*γ (Perseus Proteomics; 1:100), rabbit calbindin (Sigma; 1:1,000), and rabbit PKCα (Sigma; 1:20,000). For flat-mount immunohistochemistry, whole retinas were fixed with 4% paraformaldehyde in phosphate buffer for ∼60 min at room temperature. After 1 h blocking with 10% horse serum in PBS + 0.1% Triton ×-100, the eyecups were immunostained for 2 d with anti-Rho4D2 and S-opsin (sc-14363; Santa Cruz Biotechnology) antibodies in 1:200 and 1:500 dilution, respectively. After secondary antibody reaction, the retinas were flattened on slide glasses. Images were taken on an Apotome confocal-style 3D imaging microscope (Zeiss). In situ hybridization was performed as previously described (3).

In Vivo Electroporation. In vivo electroporation was performed at postnatal day (P) 0 as previously described (6). Approximately 0.3 μL of DNA solution (5 μg/μL) was injected into the subretinal space of P0 mouse pups, and square electric pulses (100 V; five 50-ms pulses with 950-ms intervals) were applied with tweezer-type electrodes (BTX; model 522). CAG-GFP vector was coelectroporated (1 μg/μL) with both shRNA constructs (U6-control and U6-*ERR*β) to allow for visualization of transfected cells. The electroporated retinas were harvested at P14 for immunohistochemistry.

Luciferase Analysis. Luciferase analysis was performed essentially as previously described (1). The region from −2174 to +70 of the bovine rhodopsin promoter region was used to generate the reporter, as previously described (1). An evolutionarily conserved steroid hormone-binding motif at the proximal region of the rhodopsin promoter (AGGTCA, 136 bp upstream from the start codon) was mutated to CTTTCA by a QuikChange II-XL site-directed mutagenesis kit (Stratagene).

DNA Microarray Analysis. Total RNA was extracted from retinas of P21 wild-type and *ERR*$\beta^{-/-}$ mice. A minimum of four retinas from each genotype that were independently dissected were pooled, and RNA was prepared using the RNeasy kit (Qiagen). Three independent RNA preparations were labeled and hybridized as previously described (4). Data were analyzed using the Spotfire software package (TIBCO).

Quantitative RT-PCR. The cDNAs of P21 wild-type and *ERR*$\beta^{-/-}$ mouse retinas were synthesized from total RNAs used in microarray analysis by using SuperScript III Reverse Transcriptase (Invitrogen). Quantitative RT-PCR was performed by using a DyNAmo Flash SYBR Green qPCR Kit (New England Biolabs) and a 7300 Real-Time PCR System (Applied Biosystems) according to the manufacturers' recommended protocols. Primer sets for genes examined are as set in Table S2.

Electroretinogram. Scotopic and photopic electroretinograms (ERGs) were recorded by using an Espion ERG machine (Diagnosys LLC) as previously described (5). Mice were dark-adapted more than 12 h before recording scotopic ERGs, and light-adapted at 30 cd/m^2 white light for 10 min for photopic ERGs. Scotopic ERGs were recorded at 11 intensity levels of white light ranging from −3.00 to 1.40 log cd-s/m^2. Photopic ERGs were recorded at three levels of white light (0.60, 1.00, and 1.40 log cd-s/m^2). Six to eight measurements were averaged at each flash intensity.

Retinal Explants and TUNEL Staining. P14 retinas were dissected and explanted as previously described (2). The culture media containing 0.1% EtOH (carrier), 10 μM diethylstilbestrol (DES) (Sigma), 10 μM 4-hydroxytamoxifen (4-OHT) (Sigma), and 10 μM DY131 (Tocris Bioscience) were changed every 2 d. The retinas explanted for 2 d in vitro (div 2) and 4 d in vitro (div 4) d were fixed in 4% paraformaldehyde/phosphate buffer for 30 min at room temperature. The explant sections were prepared as described in above. TUNEL staining was performed by using the In Situ Cell Death Detection Kit, TMR Red (Roche), using the manufacturer's recommended protocol.

1. Onishi A, et al. (2009) Pias3-dependent SUMOylation directs rod photoreceptor development. *Neuron* 61:234–246.
2. Matsuda T, Cepko CL (2004) Electroporation and RNA interference in the rodent retina in vivo and in vitro. *Proc Natl Acad Sci USA* 101:16–22.
3. Blackshaw S, et al. (2004) Genomic analysis of mouse retinal development. *PLoS Biol* 2:e247.
4. Chen J, Nathans J (2007) Estrogen-related receptor β/NR3B2 controls epithelial cell fate and endolymph production by the stria vascularis. *Dev Cell* 13:325–337.
5. Okoye G, et al. (2003) Increased expression of brain-derived neurotrophic factor preserves retinal function and slows cell death from rhodopsin mutation or oxidative damage. *J Neurosci* 23:4164–4172.

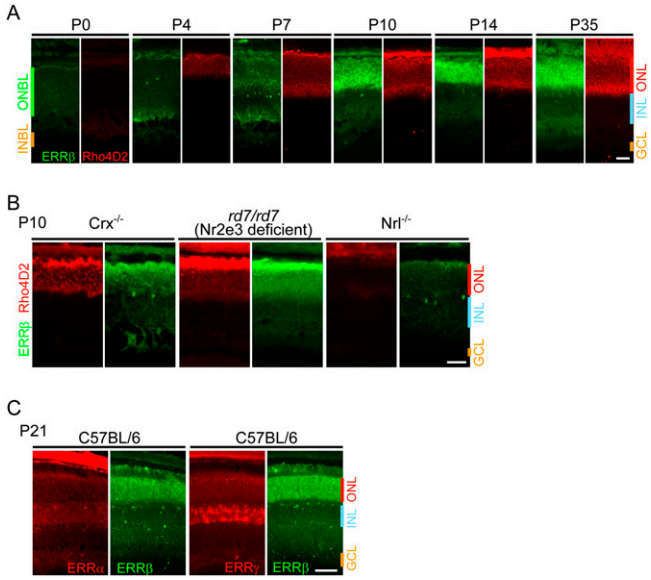

Fig. S1. (*A*) Developmental expression of *ERR*β (green) coimmunostained with Rho4D2 (red) from P0, 4, 7, 10, 14, and 35. ONBL, outer neuroblastic layer; INBL, inner neuroblastic layer; ONL, outer nuclear layer; INL, inner nuclear layer; GCL, ganglion cell layer. (Scale bar, 20 μm.) (*B*) *ERR*β expression in the mouse retina which carries mutations in photoreceptor-specific transcription factors (Crx, Nr2e3, and Nrl). *ERR*β expression is absent in *Nrl*$^{-/-}$ mice, reduced in *Crx*$^{-/-}$ mice, and essentially unaffected in Nr2e3$^{-/-}$ mice. (Scale bar, 15 μm.) (*C*) Immunostaining of other *ERR* family members, *ERR*α and *ERR*γ, in adult retina (red). (Scale bar, 15 μm.)

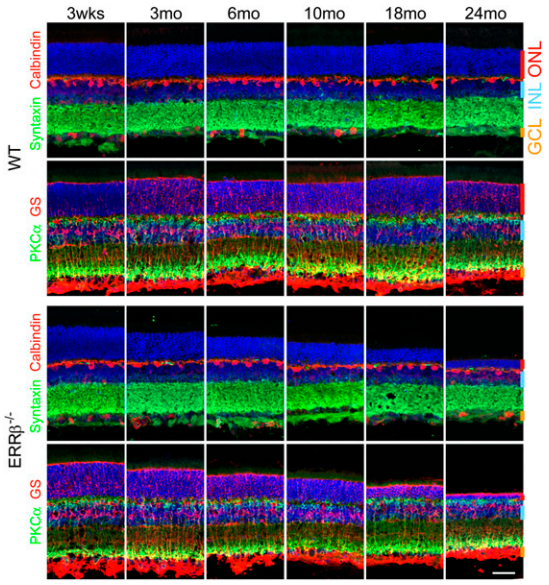

Fig. S2. No significant morphological change was observed in the inner retina of *ERR*β$^{-/-}$ mouse retina. Retinal sections of aged (P21, 3, 6, 10, 18, and 24 mo) mice were labeled with syntaxin, calbindin, PKCα, and GS as indicated. (Scale bar, 20 μm.)

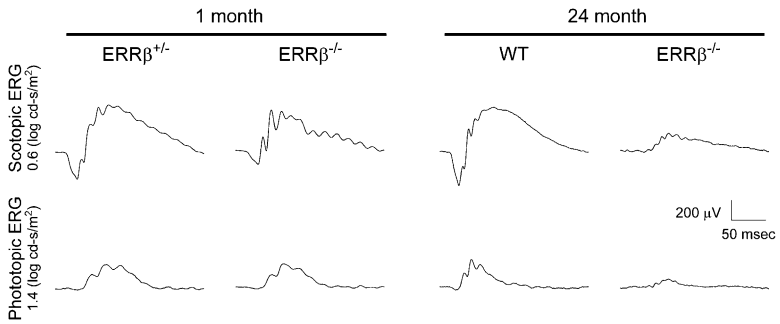

Fig. S3. (*Left*) Scotopic (rod) and photopic (cone) ERG responses from 1-mo-old *ERR*β$^{+/-}$ and *ERR*β$^{-/-}$ mice. No significant difference in amplitude of response is observed between the two genotypes. (*Right*) Scotopic (rod) and photopic (cone) ERG responses from 24-mo-old wild-type and *ERR*β$^{-/-}$ mice. A substantial deterioration of both responses is observed in *ERR*β$^{-/-}$ animals relative to wild type.

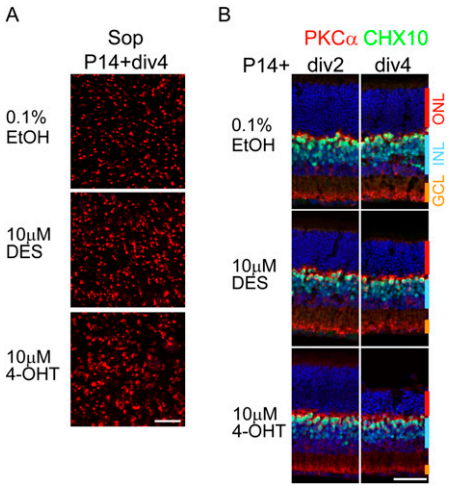

Fig. S4. *ERR*-specific inverse agonists did not affect nonrod retinal neurons. (*A*) Flat-mount immunohistochemistry of P14 + 4 d in vitro (div 4) retinas stained with S-opsin to visualize cone photoreceptors. The explants were exposed to 0.1% EtOH (carrier) and 10 μM DY131. *ERR* inverse agonists did not affect cone photoreceptors. (Scale bar, 40 μm.) (*B*) Section immunohistochemistry of P14 + div 2 and + div 4 retinal explants colabeled with the bipolar cell markers PKCα and CHX10. *ERR* inverse agonists did not affect bipolar cell morphology or survival. (Scale bar, 20 μm.)

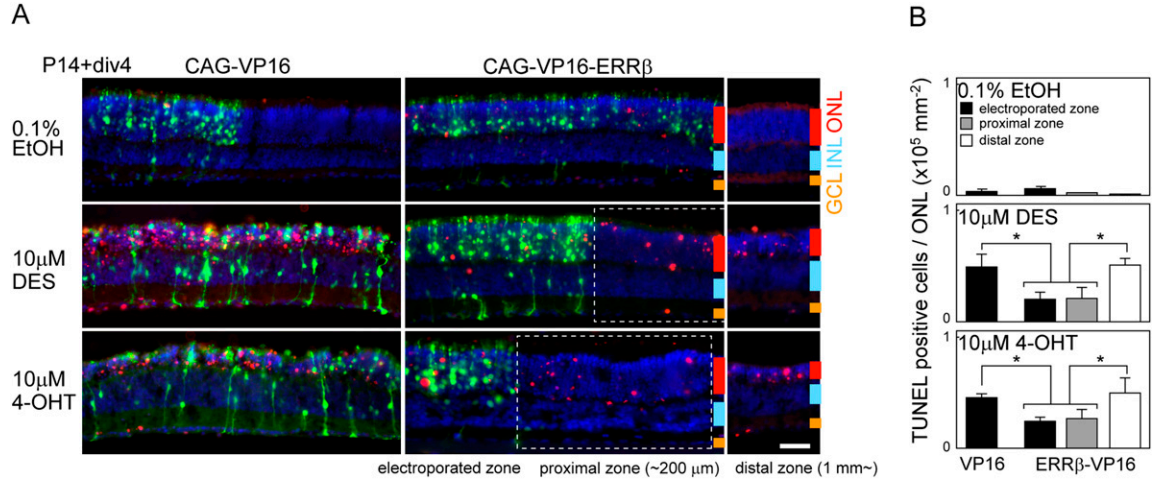

Fig. S5. Non-cell-autonomous effect of *ERR*β for maintenance and survival of rod photoreceptor cells. (*A*) TUNEL staining (red) with DAPI (blue) of P14 + div 4 retinal explants electroporated in vivo at P0 with CAG-VP16 (control) and CAG-*ERR*β-VP16 (constitutively active construct). The explants were exposed to 0.1% EtOH (carrier), 10 μM DES, and 10 μM 4-OHT. TUNEL staining is shown at the electroporated zone, the proximal nonelectroporated zone (~200 μm in distance from the electroporated zone), and the distal zone (1 mm away from the electroporated zone). (Scale bar, 20 μm.) (*B*) The fraction of TUNEL-positive cells in ONL in *A* normalized by the area of ONL. All data are represented as mean ± SD (n = 3). *P < 0.05 by Student's t test.

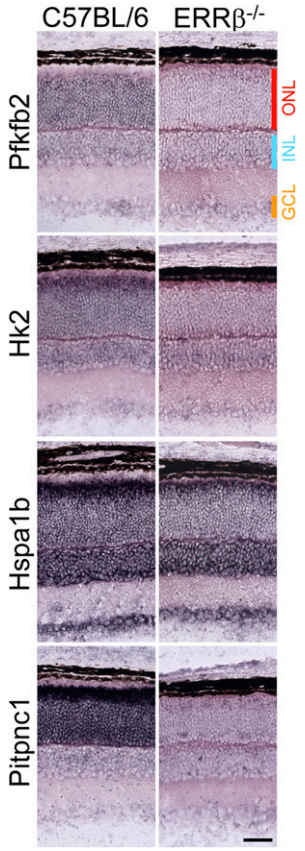

Fig. S6. In situ hybridization of P21 C57BL/6 and *ERR*β$^{-/-}$ mouse retinas visualized with four probes (Pfkfb2, Hk2, Hspa1b, and Pitpnc1) that are down-regulated in microarray analysis. (Scale bar, 20 μm.)

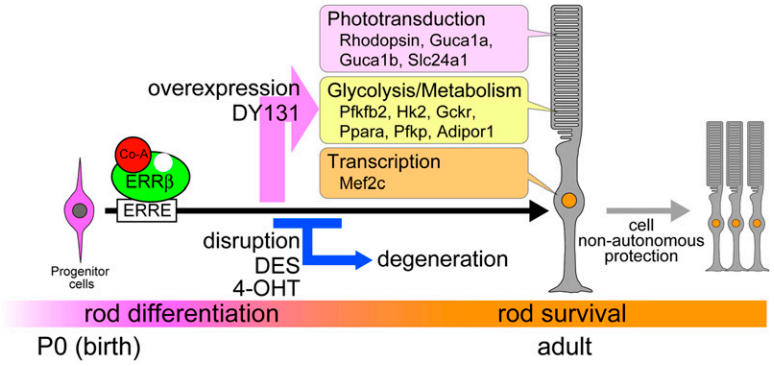

Fig. S7. Model for *ERR*β action in regulation of rod photoreceptor-specific gene expression and rod survival. From the second postnatal week onward, *ERR*β directly activates expression of genes that mediate phototransduction and energy metabolism in rod photoreceptors. *ERR*β acts through both cell-autonomous and non-cell-autonomous mechanisms to mediate cell survival. Loss of function of *ERR*β induced by either mutation or treatment of retinal explants with inverse agonists of *ERR*β results in rod photoreceptor degeneration, whereas gain of function of *ERR*β can rescue defects in photoreceptor-specific gene expression and rod photoreceptor degeneration observed in *Crx*$^{-/-}$ mice.

Table S1.

Genes	Forward primers (5′→3′)	Reverse primers (5′→3′)
Rho	CCCTTCTCCAACGTCACAGG	TGAGGAAGTTGATGGGGAAGC
Guca1a	ACCGAGTGCCATCAGTGGTAT	CTGCCACGTACTCCATGAAGT
Guca1b	GGAGGCGATTTACAAGCTGAA	GCCGTCTCCATTCTCGTCC
Aipl1	GGGTCTACCCTATGTTGTCCC	GGAAGAGGCCGCAACTCTAAA
Pfkfb2	GACAAGCCAACTCACAACTTCC	ACACTGTAATTTCTTGGACGCC
Hk2	CGAAATGTGACGTGTCCT	GTGAGGAAGCAGGGAAGT
Hspa1b	TGGTGCAGTCCGACATGAAG	GCTGAGAGTCGTTGAAGTAGGC
Pitpnc1	TATCCCTGCGATCTTGGTGTG	CCCCACTTAGATGTGAAGCCA
Adipor1	GTTTGCCACTCCCAAGCA	ACACCACTCAAGCCAAGTCC
Gckr	CCAAGCACCAAGCGGTATCA	GTCAGTGGGTTGGACTTCTCT
Mef2c	GTCAGTTGGGAGCTTGCACTA	CGGTCTCTAGGAGGAGAAACA
Pdia5	GACCCGCAATAACGTGCTG	CTCGGTCATACTGCATGTGAAA
Slc6a6	GCACACGGCCTGAAGATGA	ATTTTTGTAGCAGAGGTACGGG
Gapdh	AGGTCGGTGTGAACGGATTTG	TGTAGACCATGTAGTTGAGGTCA
Actb	GGCTGTATTCCCCTCCATCG	CCAGTTGGTAACAATGCCATGT

Table S2. Selected genes down-regulated in P21 retina of *ERRβ*$^{-/-}$ mice

Gene	*P* value	Fold change	Expression pattern	Function
Pfkfb2	0.00002	−2.91	Rod-specific*	Regulation of glycolysis
Hk2	0.0062	−2.00	Rod-enriched*	Regulation of glycolysis
Gckr	0.0057	−1.73	Photoreceptor-enriched†	Regulation of glycolysis
Pfkp	0.0498	−1.87	ND	Regulation of glycolysis
Adipor1	0.0083	−1.44	Rod-specific	Glucose and lipid metabolism
Ppara	0.0291	−3.83	Rod-enriched†	Transcription/regulation of metabolism
Guca1a	0.0033	−3.24	Rod-specific	Phototransduction
Guca1b	0.0127	−1.60	Rod-specific	Phototransduction
Slc24a1	0.0076	−1.79	Rod-specific	Phototransduction
Rho	0.0097	−1.27	Rod-specific	Phototransduction
Hspa1b	0.0085	−3.98	Rod-specific*	Protein folding/stress response
Aipl1	0.0136	−1.59	Rod-specific	Protein folding/stress response
Mef2c	0.0009	−6.55	Rod-enriched†	Transcription
Pitpnc1	0.0322	−1.49	Rod-specific*	Phosphoinositide synthesis

The results of three biological replicate hybridizations are shown for both genotypes. The $\log_2$ mean signal intensity is shown for each probe, along with the linear fold change and computed unpaired *P* value for differential expression. Where the cellular expression pattern of the transcript in question was previously known, it is indicated, along with the relevant reference. "Specific" indicates that the transcript is exclusively expressed in rod photoreceptors; "enriched" indicates that the transcript is substantially more highly expressed in rod photoreceptors than in other retinal cell types (or is inferred to be, based on down-regulation in Nrl$^{-/-}$ retinas); "widespread" indicates that the transcript is ubiquitously expressed; "inner retina" indicates that the transcript is selectively expressed in nonphotoreceptor cell types of the inner nuclear layer and/or ganglion cell layer; and "cones" indicates predominant expression in cone photoreceptors. ND, not determined.

*Gene expression patterns characterized in this study (Fig. S6).

†Genes significantly down-regulated in Nrl$^{-/-}$ mice, but whose cellular expression pattern has not yet been directly investigated.

Other Supporting Information Files

Dataset S1 (TXT)